



Short communication: Inverse isochron regression for Re–Os, K–Ca and other chronometers

Yang Li¹ and Pieter Vermeesch²

¹State Key Laboratory of Lithospheric Evolution, Institute of Geology and Geophysics, Chinese Academy of Sciences, Beijing 100029

²Department of Earth Sciences, University College London, Gower Street, London WC1E 6BT

Correspondence: Pieter Vermeesch (p.vermeesch@ucl.ac.uk)

Abstract. Conventional Re–Os isochrons are based on mass spectrometric estimates of $^{187}\text{Re}/^{188}\text{Os}$ and $^{187}\text{Os}/^{188}\text{Os}$. ^{188}Os is usually far less abundant, and is therefore measured less precisely, than ^{187}Os and ^{187}Re . This causes strong error correlations between the two isochron ratios, which may obscure potentially important geological complexity. Using an approach that is widely accepted in $^{40}\text{Ar}/^{39}\text{Ar}$ and U–Pb geochronology, we here show that these error correlations are greatly reduced by applying a simple change of variables, using ^{187}Os as a common denominator. Plotting $^{188}\text{Os}/^{187}\text{Os}$ vs. $^{187}\text{Re}/^{187}\text{Os}$ produces an ‘inverse isochron’, defining a binary mixing line between an inherited Os-component whose $^{188}\text{Os}/^{187}\text{Os}$ -ratio is given by the vertical intercept, and the radiogenic $^{187}\text{Re}/^{187}\text{Os}$ -ratio, which corresponds to the horizontal intercept. Inverse isochrons facilitate the identification of outliers and other sources of data dispersion. They can also be applied to other geochronometers such as the K–Ca method and (with less dramatic results) the Rb–Sr, Sm–Nd and Lu–Hf methods. The generalised inverse isochron method has been added to the `IsoplotR` toolbox for geochronology, which automatically converts conventional isochron ratios into inverse ratios and vice versa.

1 Introduction: the conventional Re–Os isochron

The Re–Os method is based on the β -decay of ^{187}Re to ^{187}Os :

$$^{187}\text{Os} = ^{187}\text{Os}_i + ^{187}\text{Re} (\exp[\lambda_{187}t] - 1) \quad (1)$$

where λ_{187} is the decay constant of ^{187}Re ($= 0.01666 \times 0.00017 \text{ Gyr}^{-1}$, Smoliar et al., 1996), t is the time elapsed since isotopic closure, and $^{187}\text{Os}_i$ is the inherited (non-radiogenic) ^{187}Os -component. Because both t and $^{187}\text{Os}_i$ are generally unknown, Equation 1 is underdetermined. This problem can be solved by analysing multiple cogenetic aliquots and normalising both sides of Equation 1 to non-radiogenic ^{188}Os :

$$\left[\frac{^{187}\text{Os}}{^{188}\text{Os}} \right] = \left[\frac{^{187}\text{Os}}{^{188}\text{Os}} \right]_i + \left[\frac{^{187}\text{Re}}{^{188}\text{Os}} \right] (\exp[\lambda_{187}t] - 1) \quad (2)$$

Equation 2 forms the equation of a line:

$$y = a + bx \quad (3)$$



where $x = [^{187}\text{Re}/^{188}\text{Os}]$, $y = [^{187}\text{Os}/^{188}\text{Os}]$, $a = [^{187}\text{Os}/^{188}\text{Os}]_i$, and $b = (\exp[\lambda_{187}t] - 1)$. Both the independent variable (x) and the dependent variable (y) are associated with analytical uncertainty. Therefore, linear regression of the isochron line is typically done by weighted least squares regression with uncertainty in both variables (York et al., 2004).

25 One problem with the conventional isochron definition of Equation 2 is that the rarest isotope, ^{188}Os , which is associated with the largest mass spectrometer uncertainties, appears in the denominator of both x and y . This has the potential to produce strong spurious error correlations (Pearson, 1896). For example, consider the following hypothetical (independent) abundance estimates:

$$X \equiv ^{187}\text{Os} = 2,000 \pm 10 \text{ fmol}; Y \equiv ^{187}\text{Re} = 30,000 \pm 50 \text{ fmol and } Z \equiv ^{188}\text{Os} = 10 \pm 2 \text{ fmol}$$

30 then the ($^{187}\text{Os}/^{188}\text{Os}$) and ($^{187}\text{Re}/^{188}\text{Os}$) isotope ratio estimates exhibit a correlation coefficient of

$$\rho_{\frac{X}{Z}, \frac{Y}{Z}} \approx \frac{\left(\frac{s[Z]}{Z}\right)^2}{\sqrt{\left(\frac{s[Y]}{Y}\right)^2 + \left(\frac{s[Z]}{Z}\right)^2} \sqrt{\left(\frac{s[X]}{X}\right)^2 + \left(\frac{s[Z]}{Z}\right)^2}} = \frac{\left(\frac{2}{10}\right)^2}{\sqrt{\left(\frac{50}{30,000}\right)^2 + \left(\frac{2}{10}\right)^2} \sqrt{\left(\frac{10}{2,000}\right)^2 + \left(\frac{2}{10}\right)^2}} = 0.9997 \quad (4)$$

The strong error correlation between the two variables on the isochron diagram are manifested as narrow and steeply inclined error ellipses, which may graphically obscure any geologically significant trend.

As an example, consider the Re–Os dataset of Morelli et al. (2007) (Figure 1a). At first glance, this dataset appears to define
 35 an excellent isochron with a clear slope corresponding to an isochron age of 287 Ma. However upon closer inspection, the interpretation of this fit is not so simple:

1. The isochron fit exhibits an MSWD of 2.5, which indicates the presence of a moderate amount of overdispersion of the data with respect to the formal analytical uncertainties. It is not immediately clear which aliquots are responsible for the poor goodness-of-fit.
- 40 2. The error ellipses exhibit a tremendous range of sizes. The plot is dominated by the least precise measurement (i.e. aliquot 14), and the remaining aliquots are barely visible.
3. The error ellipses are nearly perfectly aligned with the isochron, which makes it difficult to distinguish between geochronologically significant and statistically spurious sources of correlation.

2 The inverse Re–Os isochron

45 All three of these problems can be solved by a simple change of variables:

$$\left[\frac{^{188}\text{Os}}{^{187}\text{Os}}\right] = \left[\frac{^{188}\text{Os}}{^{187}\text{Os}}\right]_i \left\{ 1 - \left[\frac{^{187}\text{Re}}{^{187}\text{Os}}\right] (\exp[\lambda_{187}t] - 1) \right\} \quad (5)$$

which defines an ‘inverse’ isochron line:

$$y' = a' + b'x' \quad (6)$$

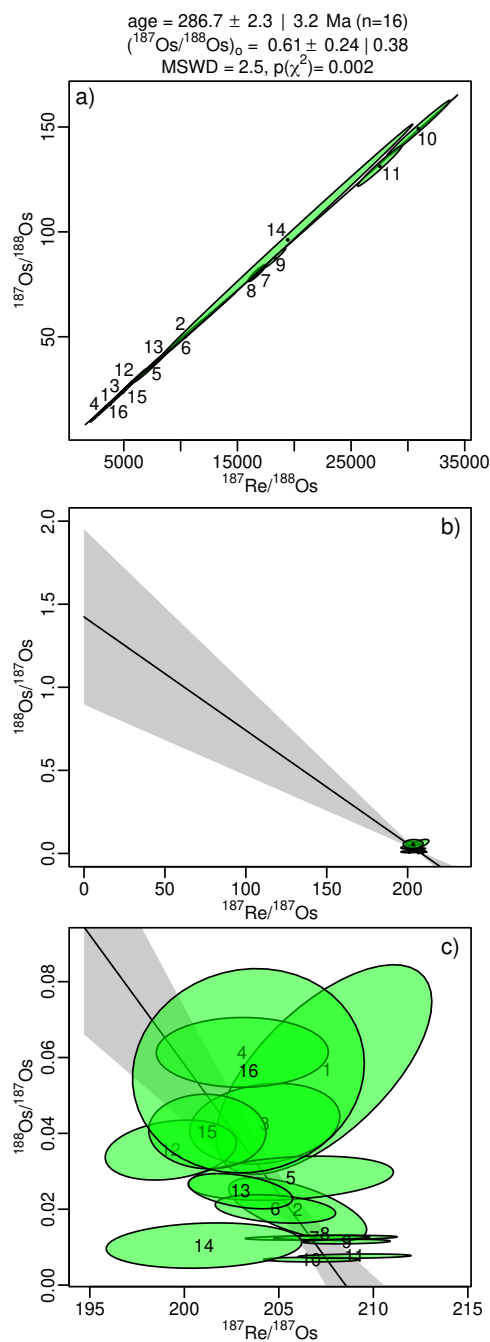


Figure 1. a) conventional isochron of the Re–Os data of Morelli et al. (2007), with uncertainties shown as 95% confidence intervals without and with $\sqrt{\text{MSWD}}$ overdispersion multiplier. b) and c) the inverse isochron diagram of the same data represents a mixing line between inherited and radiogenic components. The sample is highly radiogenic, allowing precise age estimation despite the presence of significant overdispersion, which is masked by the error correlations in the conventional isochron diagram. All error ellipses are shown at 95% confidence. The grey confidence envelopes represent the standard error of the fit ignoring the overdispersion.



where $x' = [^{187}\text{Re}/^{187}\text{Os}]$, $y' = [^{188}\text{Os}/^{187}\text{Os}]$, $a' = [^{188}\text{Os}/^{187}\text{Os}]_i$, and $b' = -[^{188}\text{Os}/^{187}\text{Os}]_i (\exp[\lambda_{187}t] - 1)$.

50 Equation 5 defines a mixing line between the non-radiogenic $[^{188}\text{Os}/^{187}\text{Os}]$ -ratio (which marks the vertical intercept) and the radiogenic $[^{187}\text{Re}/^{187}\text{Os}]$ -ratio (which marks the horizontal intercept). By moving the least abundant nuclide to the numerator of the dependent variable, instead of the denominator of both the dependent and the independent variables, the inverse isochron reduces the error correlations. Revisiting the earlier hypothetical example yields an error correlation of:

$$\rho_{\frac{Y}{X} \frac{Z}{X}} \approx \frac{\left(\frac{s[X]}{X}\right)^2}{\sqrt{\left(\frac{s[X]}{X}\right)^2 + \left(\frac{s[Y]}{Y}\right)^2} \sqrt{\left(\frac{s[X]}{X}\right)^2 + \left(\frac{s[Y]}{Y}\right)^2}} = \frac{\left(\frac{10}{2,000}\right)^2}{\sqrt{\left(\frac{10}{2,000}\right)^2 + \left(\frac{50}{30,000}\right)^2} \sqrt{\left(\frac{10}{2,000}\right)^2 + \left(\frac{2}{10}\right)^2}} = 0.024 \quad (7)$$

55 Plotting the dataset of Morelli et al. (2007) on an inverse isochron diagram provides a much clearer picture of it (Figure 1b and c):

1. The overdispersion is clearly visible and can be attributed to aliquots 1, 12 and 14. Most of the geochronologically valuable information is contained in the highly radiogenic aliquots 7–11, which tightly cluster near the $[^{187}\text{Re}/^{187}\text{Os}]$ -intercept. Even though the data are overdispersed, the overall composition is very radiogenic and can therefore be used to obtain precise age constraints. The initial $[^{187}\text{Os}/^{188}\text{Os}]$ -ratio, however, is poorly constrained.
2. Although the error ellipses still exhibit a range of sizes, reflecting the heteroscedasticity of the data, the imprecise measurements do no longer dominate the plot to the extent where they obscure the precise ones.
3. The error ellipses are no longer aligned parallel to the isochron line, but are oriented at an angle to it. This makes it easier to see the difference between the geochronological and statistical sources of correlation.

65 3 Application to other chronometers

Inverse isochron ratios, in which the radiogenic daughter isotope is used as a common denominator, are frequently used in $^{40}\text{Ar}/^{39}\text{Ar}$ (Turner, 1971) and U–Pb (Tera and Wasserburg, 1972) geochronology. They are equally applicable to other dating methods, such as Rb–Sr ($[^{87}\text{Sr}/^{86}\text{Sr}]$ vs. $[^{87}\text{Rb}/^{86}\text{Sr}]$), Sm–Nd ($[^{144}\text{Nd}/^{143}\text{Nd}]$ vs. $[^{147}\text{Sm}/^{143}\text{Nd}]$), Lu–Hf ($[^{177}\text{Hf}/^{176}\text{Hf}]$ vs. $[^{176}\text{Lu}/^{176}\text{Hf}]$) and K–Ca ($[^{44}\text{Ca}/^{40}\text{Ca}]$ vs. $[^{40}\text{K}/^{40}\text{Ca}]$). In the case of K–Ca dating, the inverse approach offers similar benefits as for the Re–Os method because ^{44}Ca is typically 100 times less abundant than ^{40}Ca , thus making the conventional isochron plot prone to strong error correlations (Figure 2). For other chronometers such as Rb–Sr, Sm–Nd and Lu–Hf, whose non-radiogenic isotopes are at least as abundant as the radiogenic daughter isotopes, the benefits of the inverse isochron approach are less obvious.

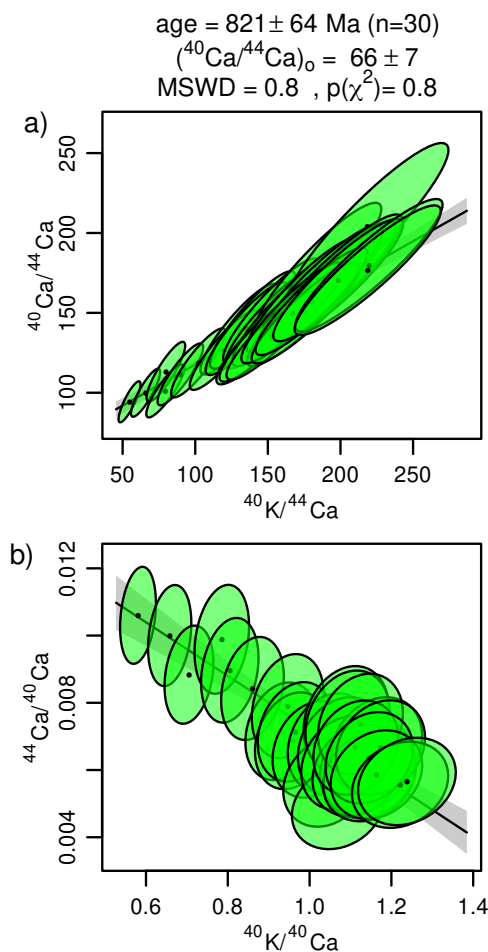


Figure 2. a) conventional and b) inverse isochron of the K–Ca data for spot 5 of Harrison et al. (2010)’s sample 140025h, which forms a well defined isochron without overdispersion.

Given a data table of conventional isochron ratios (x and y in Equation 3), it is possible to calculate the inverse ratios (x' and y' in Equation 6), their uncertainties ($s[x']$ and $s[y']$) and error correlations ($\rho_{x'y'}$) using the following equations:

$$\begin{cases} x' = \frac{x}{y} \\ y' = \frac{1}{y} \\ \left(\frac{s[x']}{x'}\right)^2 = \left(\frac{s[x]}{x}\right)^2 - 2\rho_{x,y} \left(\frac{s[x]}{x}\right) \left(\frac{s[y]}{y}\right) + \left(\frac{s[y]}{y}\right)^2 \\ \left(\frac{s[y']}{y'}\right)^2 = \left(\frac{s[y]}{y}\right)^2 \\ \rho_{x'y'} = \left(\frac{x'}{s[x']}\right) \left[\left(\frac{y}{s[y]}\right) - \rho_{xy} \left(\frac{x}{s[x]}\right)\right] \end{cases} \quad (8)$$



This transformation is perfectly symmetric in the sense that it can also be used to convert inverse isochron ratios to conventional ones. To do this, it suffices to swap x' and y' for x and y and vice versa.

4 Implementation in IsoplotR

80 Inverse isochrons have been added to all the relevant chronometers in the `IsoplotR` toolbox for radiometric geochronology (Vermeesch, 2018). This functionality can be used either from the graphical user interface (which can be accessed both online and offline, Figure 3a), or from the command line, using the R programming language and application programming interface (Figure 3b and c). `IsoplotR` automatically executes the ratio conversion of Equation 8 in the background, so the user can supply their data as conventional ratios and still plot them on an inverse isochron diagram.

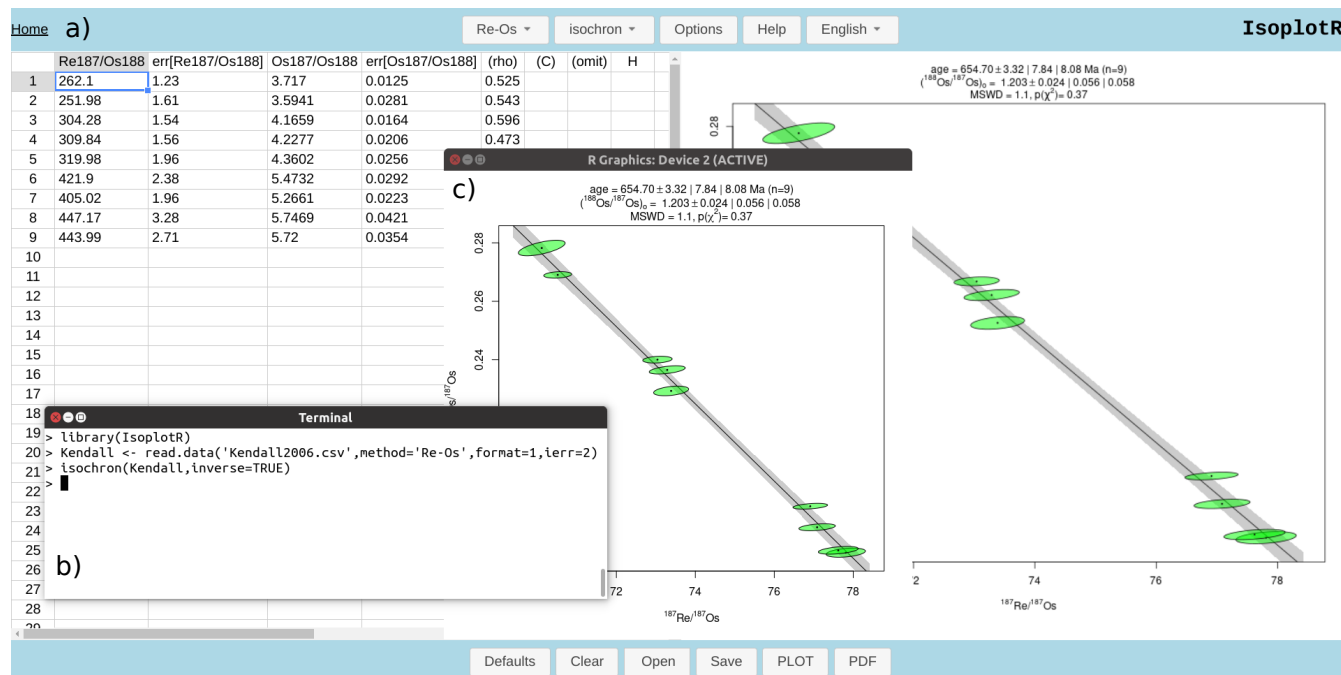


Figure 3. Inverse isochrons can be constructed with `IsoplotR`, either using its graphical user interface (a), or from the R command prompt (b). Both options produce the same graphical and numerical output, shown here for a Re–Os dataset of Kendall et al. (2006) (c).

85 5 Conclusions

Conventional isochrons are straight line regressions between two ratios D/d and D/P , where P and D are the parent and daughter nuclides, and d is a non-radiogenic isotope of the daughter element. This paper reviewed the phenomenon whereby strong error correlations arise when d is less abundant than D , and is therefore measured less precisely than D . This is the case



90 in Re–Os and K–Ca geochronology, which use ^{188}Os and ^{44}Ca as normalising isotopes, respectively. These isotopes are tens to
hundreds of times less abundant than the radiogenic ^{187}Os and ^{40}Ca . Note that some K–Ca studies use ^{42}Ca as a normalising
isotope, which is even less abundant ^{44}Ca , and therefore further aggravates the problem.

The spurious correlation between the isochron ratio measurements can be so strong ($r > 0.99$) that it outweighs and obscures
the geochronological correlation. This is not only inconvenient from an esthetic point of view, but may also cause numerical
problems. It is not uncommon for data tables to either not report error correlations at all, or to report them to only one significant
95 digit. However, the difference between error correlations of $r = 0.991$ and $r = 0.999$, say, may have a large effect on the
isochron age. All these problems can be solved by recasting the isochron regression into a new form, by plotting d/D vs. P/D .
This produces a different type of linear trend, in which the vertical intercept yields the reciprocal daughter ratio, and the age is
not proportional to the slope of the isochron line, but inversely proportional to its horizontal intercept. The two formulations
are mathematically equivalent (Dalrymple et al., 1988) provided that the relative uncertainties of the ratio measurements are
100 reasonably small ($< 10\%$, say).

Code and data availability. IsoplotR is free software released under the GPL-3 license. The package and its source code are available
from <https://cran.r-project.org/package=IsoplotR>.

Author contributions. PV wrote the software and the paper. YL formulated the research question and contributed to the writing of the paper.

Competing interests. Pieter Vermeesch is an associate editor of *Geochronology*.

105 *Acknowledgements.* We thank David Selby for feedback on an early version of the manuscript. This research was supported by National Key
Research and Development Program of China grant #2018YFA0702600 and National Natural Science Foundation of China grant #42022022
awarded to YL; and by NERC standard grant #NE/T001518/1 ('Beyond Isoplot') awarded to PV.



References

- 110 Dalrymple, G. B., Lanphere, M. A., and Pringle, M. S.: Correlation diagrams in $^{40}\text{Ar}/^{39}\text{Ar}$ dating: Is there a correct choice?, *Geophysical Research Letters*, 15, 589–591, 1988.
- Harrison, T. M., Heizler, M. T., McKeegan, K. D., and Schmitt, A. K.: In situ ^{40}K – ^{40}Ca ‘double-plus’ SIMS dating resolves Klokken feldspar ^{40}K – ^{40}Ar paradox, *Earth and Planetary Science Letters*, 299, 426–433, 2010.
- Kendall, B., Creaser, R. A., and Selby, D.: Re–Os geochronology of postglacial black shales in Australia: Constraints on the timing of “Sturtian” glaciation, *Geology*, 34, 729–732, 2006.
- 115 Morelli, R., Creaser, R. A., Seltmann, R., Stuart, F. M., Selby, D., and Graupner, T.: Age and source constraints for the giant Muruntau gold deposit, Uzbekistan, from coupled Re–Os–He isotopes in arsenopyrite, *Geology*, 35, 795–798, 2007.
- Pearson, K.: Mathematical contributions to the theory of evolution.—on a form of spurious correlation which may arise when indices are used in the measurement of organs, *Proceedings of the Royal Society of London*, 60, 489–498, 1896.
- Smoliar, M. I., Walker, R. J., and Morgan, J. W.: Re–Os ages of group IIA, IIIA, IVA, and IVB iron meteorites, *Science*, 271, 1099–1102, 120 1996.
- Tera, F. and Wasserburg, G.: U–Th–Pb systematics in three Apollo 14 basalts and the problem of initial Pb in lunar rocks, *Earth and Planetary Science Letters*, 14, 281–304, 1972.
- Turner, G.: ^{40}Ar – ^{39}Ar ages from the lunar maria, *Earth and Planetary Science Letters*, 11, 169–191, 1971.
- Vermeesch, P.: *IsoplotR*: a free and open toolbox for geochronology, *Geoscience Frontiers*, 9, 1479–1493, 2018.
- 125 York, D., Evensen, N. M., Martínez, M. L., and De Basabe Delgado, J.: Unified equations for the slope, intercept, and standard errors of the best straight line, *American Journal of Physics*, 72, 367–375, 2004.